ISSN 0020-1685, Inorganic Materials, 2012, Vol. 48, No. 5, pp. 469–475. © Pleiades Publishing, Ltd., 2012.
Original Russian Text © T.V. Plakhova, M.V. Shestakov, A.N. Baranov, 2012, published in Neorganicheskie Materialy, 2012, Vol. 48, No. 5, pp. 549–556.

# Effect of Textured Seeds on the Morphology and Optical Properties of Solution- and Vapor-Grown ZnO Nanorod Arrays

**T. V. Plakhova, M. V. Shestakov, and A. N. Baranov**

*Moscow State University, Moscow, 119899 Russia*

*e-mail: anb@inorg.chem.msu.ru*

Received December 1, 2011

**Abstract**—This paper examines the growth of aligned ZnO nanorod arrays through chemical deposition from solution and the vapor phase. The nanorod alignment is ensured primarily by a thin layer of seeds—zinc oxide nanoparticles produced by decomposing zinc acetate directly on the substrate and aligned with their *c* axes normal to the substrate surface. The acetate route was used to produce nanorod arrays 1 × 1 mm in dimensions on substrates with photoresist.

**DOI:** 10.1134/S0020168512050135

## INTRODUCTION

In the past decade, quasi-one-dimensional zinc oxide nanostructures (rods, filaments, wires, ribbons, and others [1]) have been used to develop a variety of semiconductor devices: solar cells [2], piezoelectric nanogenerators [3], UV light emitting diodes, and gas sensors [4]. Increasing interest in this material is motivated by its unique semiconducting properties: ZnO has a wide band gap (3.37 eV) and a record-high exciton binding energy (60 meV).

The greatest potential for practical application is offered by zinc oxide nanorods grown along the normal to the substrate in the form of an array uniform in height and spacing. A layer of such nanorods has a large specific surface area, high electron mobility along their axis [5], and a number of other advantages. In contrast to epitaxial films, nanorod arrays do not suffer mechanical stress, which otherwise might have a deleterious effect on their optical and transport properties. Such structures can be combined with flexible polymer substrates, which makes such devices competitive with conventional semiconductor structures.

A number of approaches have been proposed for the synthesis of ZnO nanorod arrays: thermal growth from salt mixtures [6], sol–gel processes [7], pulsed laser deposition [8], chemical vapor deposition [9], various solution techniques [10], and others. In most of these techniques, an important part is played by surface preparation for nanorod growth. The shape of an individual ZnO nanocrystal and the orientation of the array as a whole are very sensitive to the growth surface condition. Controlled deposition onto a substrate can be ensured by seeds in the form of zinc oxide nanoparticles less than 20 nm in size, applied to the substrate surface. Despite the "random" crystallographic orientation of such nanoparticles on the substrate, the resulting nanorod array turns out to be ordered. The reason for this is that the growth of horizontally oriented crystals is suppressed by the crystallites that grow vertically. At the same time, the poorly oriented polycrystalline layer that forms in the initial stages of the process has lower structural perfection in comparison with nanorods. The boundaries between the nanoparticles in this layer act as carrier traps, reducing the electron and hole mobilities in the film and degrading its luminescent properties.

Greene et al. [11] described a technique for producing oriented seeds in the form of closely spaced nanoparticles (25–40 atomic layers) with a preferential *c*-axis orientation. Such particles do not grow epitaxially, so their oriented state cannot be accounted for in terms of crystal-chemical substrate–seed match. It is reasonable to assume that seed texturing is caused by the acetate decomposition process.

In this work, we examine the influence of such seeds on the morphology and optical properties of solution- and vapor-grown ZnO nanorods. *c*-Axis-oriented seeds were produced by decomposing zinc acetate on silicon. In addition, we demonstrate the possibility of local ZnO nanorod growth on a substrate having a photoresist mask. Such a procedure can be used in the fabrication of integrated circuits and various optoelectronic devices based on ZnO nanorods.

## EXPERIMENTAL

### *Synthesis of ZnO Nanoseeds*

To produce a uniform seed layer, we prepared a 0.005 M $Zn(CH_3COO)_2 \cdot 2H_2O$ solution in absolute ethanol. A drop of the solution was applied to a substrate rotating at 300–500 rpm. After ethanol vaporization, the substrate surface had a uniform zinc acetate layer less than 30 nm in thickness, which was air-annealed at temperatures from 250 to 350°C for 2 h.

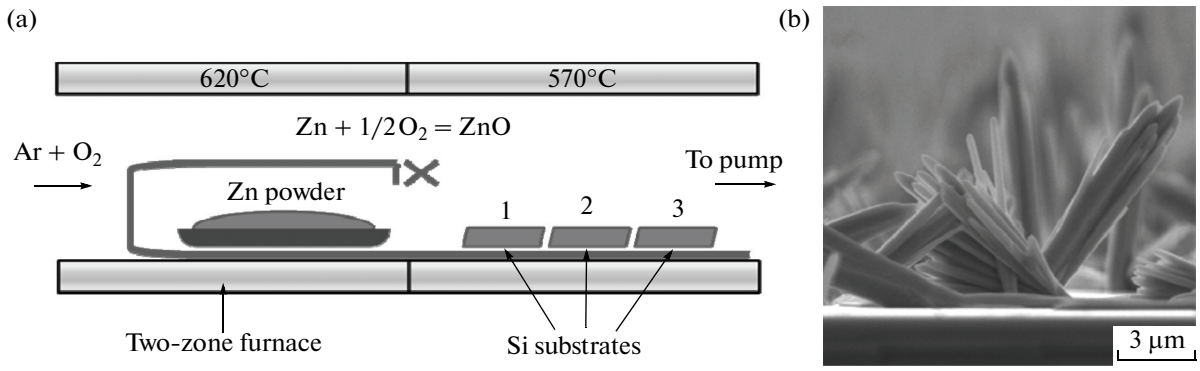


**Fig. 1.** (a) Arrangement of substrates in the reactor and (b) SEM micrograph of ZnO crystals grown from solution without seeding.

To produce local zinc oxide zones on a substrate, the following patterning procedure was used: A Microposit S1818 photoresist mask was produced on a silicon substrate by photolithography. After applying a drop of an aqueous 0.05 M $Zn(CH_3COO)_2 \cdot H_2O$ solution, the substrate was spun up to 300–500 rpm. The substrate, covered with a uniform zinc acetate layer, was dried in a drying oven for 10 min at $t = 110$°C. Next, the photoresist was dissolved away in dimethylformamide (DMFA), and the sample was annealed at $t = 350$°C. According to reference data [12], zinc acetate does not dissolve in DMFA. The photoresist should be removed in the acetate film growth step because subsequent annealing, which is needed to decompose the acetate to zinc oxide and requires a rather high temperature, may lead to photoresist polymerization. As a result of the above procedure, the substrate is covered with local regions of ZnO nanoseeds.

### *Nanorod Growth*

**Chemical precipitation from solution.** To a reaction beaker was added 3 ml of a 20% aqueous ethylenediamine ($NH_2CH_2CH_2NH_2$) solution. An aqueous 0.2 M $Zn(CH_3COOH)_2$ solution was added dropwise with constant stirring to the ethylenediamine solution until pH 8.6 was reached. Next, samples with ZnO seeds were immersed in the resultant mixture. The reaction vessel was closed and placed for 2 h in a drying oven maintained at 80–110°C. After the synthesis reached completion, the samples were carefully washed with distilled water and dried in air.

**Chemical vapor deposition.** A quartz reactor was placed in a two-zone tube furnace. A holder containing three silicon substrates and a boat with zinc powder was placed in the reactor (Fig. 1a). The holder was mounted so that the alundum boat with zinc was in zone 1 and the silicon substrates were in zone 2. The distance between the boat and the first substrate was 2 cm, and the spacing between the substrates was 1 cm. The reactor was rough-pumped for 1 h. Next, argon was admitted to the reactor, and the first and second zones were heated to their working temperatures, 620 and 570°C, respectively. After the working temperatures were reached, oxygen was introduced into the system. The fraction of oxygen in the gas mixture was 25 vol %. The synthesis was conducted for 20 min. The process parameters were selected based on previous results [13].

### *Characterization of the Nanorods*

The morphology of the samples obtained was examined by scanning electron microscopy (SEM) on a LEO Supra 50 VP. The phase composition of the samples was determined by X-ray diffraction (XRD) on a Rigaku D/MAX 2500 diffractometer ($CuK_\alpha$ radiation, rotating-anode X-ray tube). The decomposition temperature of zinc acetate was determined by differential thermal analysis (DTA) and thermogravimetry (TG) using a PerkinElmer Model Diamond TG/DTA thermoanalytical system. Photoluminescence spectra were measured on a Renishaw Raman Microscope microspectrometer. Excitation was provided by a frequency-doubled argon laser (244 nm). The spectra were recorded in a backscatter geometry using 15× and 40× laser-transparent objectives. An intensity calibration plot was obtained using the spectrum of a quartz lamp: we plotted the ratio of the integrated intensities of lines in the range 350–800 nm for the spectrum of the lamp recorded on the Raman spectrometer and on an OceanOptics spectrometer. Peak positions were calibrated using the spectrum of $Tb(bz)_3 \cdot H_2O$, reported by Kotova et al [14].

## RESULTS AND DISCUSION

### *Unseeded Nanorod Growth on Substrates*

Without seeds, zinc oxide was deposited in an uncontrolled way. When the critical supersaturation was reached, heterogeneous growth centers were formed on the substrate surface, and then crystals poorly oriented relative to the surface grew. Figure 1b shows an SEM micrograph of zinc oxide nanocrystals

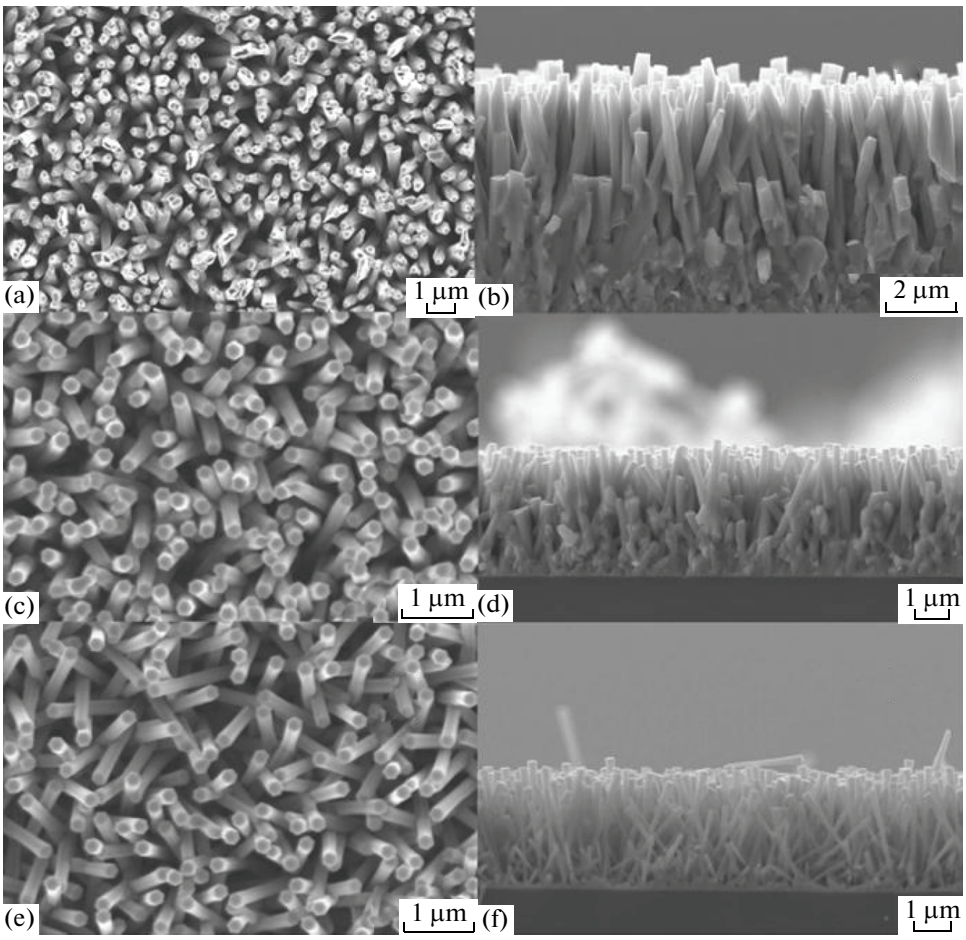


**Fig. 2.** SEM micrographs of samples obtained at different substrate–source distances (without seeding): (a) substrate in position 1 (top view), (b) substrate in position 1 (fracture surface), (c) substrate in position 2 (top view), (d) substrate in position 2 (fracture surface), (e) substrate in position 3 (top view), (f) substrate in position 3 (fracture surface).

grown on a silicon substrate without seeds. Nanocrystals grow at various angles to the surface, are poorly faceted, and differ in shape.

In the chemical vapor deposition process, the position of the substrate relative to the zinc source has a strong effect on the faceting and size of nanorods. Figure 2 shows SEM micrographs of ZnO nanorods grown on substrates without seeding. With increasing substrate–source distance, the nanorod height decreases. The nanorod length decreases from 7 to 3 μm in going from substrate 1 to substrate 3. We measured the diameter of 100 rods in a micrograph and averaged the results. It was found that the nanorods of the substrate in position 1 had the largest diameter: 420 ± 110 nm. The nanorods grown on the substrates in positions 2 and 3 had roughly the same diameter: 220 ± 30 and 215 ± 25 nm, respectively. None of the samples can be considered monodisperse.

It is worth noting the formation of a polycrystalline zinc oxide layer in the samples in positions 1 and 2. Red'kin et al. [13] interpret the formation of such a layer in terms of the competition between two zinc oxide deposition mechanisms. They believe that nanorods grow by the vapor–liquid–solid (VLS) mechanism, whereas the polycrystalline layer forms from solid zinc oxide particles that arrive to the substrate from the vapor phase (VS mechanism).

### *Zinc Acetate Decomposition*

Zinc acetate decomposition is a multistep process. Figure 3a shows the TG and DTA curves of $Zn(CH_3COO)_2 \cdot 2H_2O$.

The first step, near 100°C, is the removal of the water of crystallization, as evidenced by the step in the TG curve and the endothermic peak in the DTA curve, due to the dehydration of the crystalline hydrate:

$$Zn(CH_3COO)_2 \cdot 2H_2O \rightarrow Zn(CH_3COO)_2 + 2H_2O. \quad (1)$$

The largest weight loss takes place in the range 250–330°C. The anhydrous acetate is stable up to 250°C. Above this temperature, it decomposes to form zinc tetraoxyacetate [15], whose molecular structure

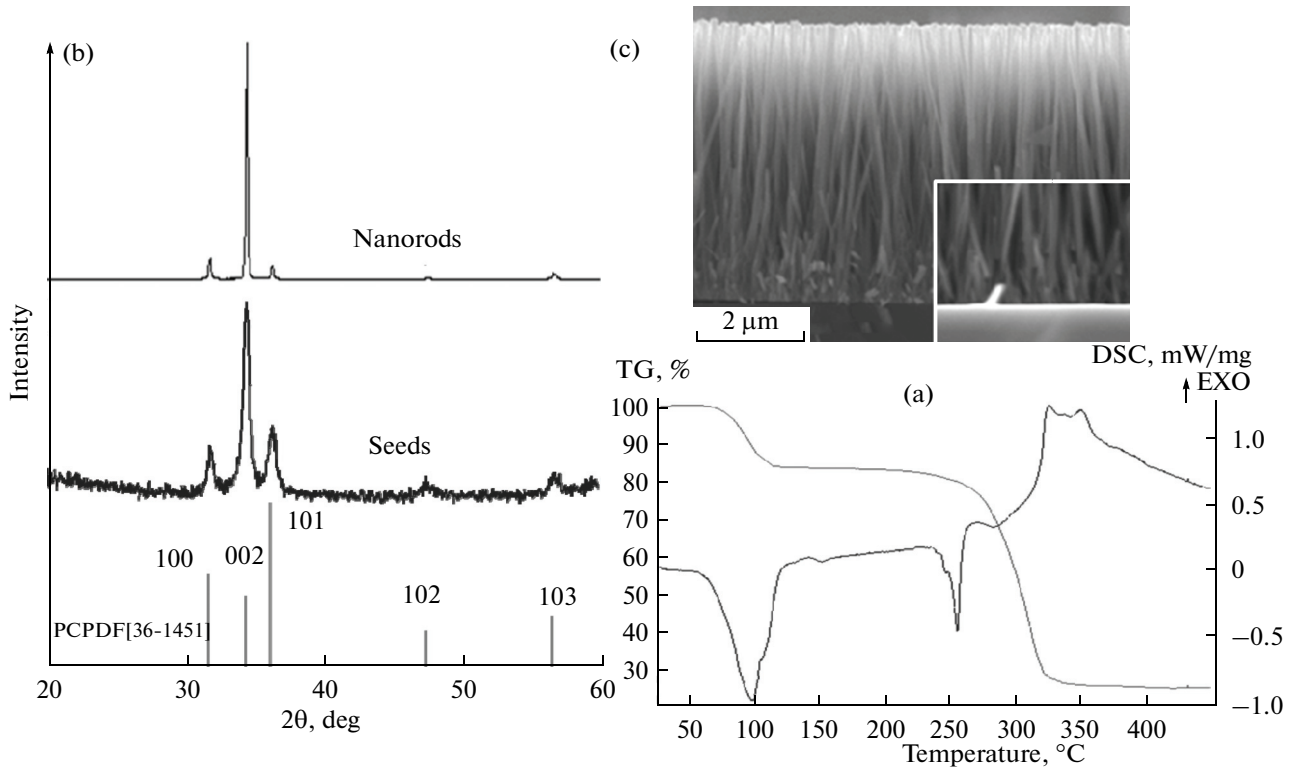


**Fig. 3.** (a) TG and DTA curves of $Zn(CH_3COO)_2 \cdot 2H_2O$; (b) XRD patterns; (c) SEM micrograph of nanorods grown from solution on seeds.

contains bridging acetate groups, like that of beryllium tetraoxyacetate [16]:

$$4Zn(CH_3COO)_2 \rightarrow Zn_4O(CH_3COO)_6 + (CH_3CO)_2O. \quad (2)$$

Zinc tetraoxyacetate has a nonpolar structure and sublimes starting above 250°C, which is accompanied by a weight loss. At the same time, the DTA curve shows a large endotherm near 260°C, which is attributable to the melting of zinc tetraoxyacetate. The decomposition of the tetraoxyacetate to ZnO reaches completion at 300–330°C [17], with a large exotherm in the DTA curve (Fig. 3a):

$$Zn_4O(CH_3COO)_6 \rightarrow 4ZnO + 3CH_3COCH_3 + 3CO_2. \quad (3)$$

The weight loss stops near 330°C. The weight loss calculated for reactions (1)–(3) is 37%, whereas the measured weight loss was 25%. The discrepancy is attributable to the high volatility of zinc tetraoxyacetate.

XRD examination of a seed layer on a substrate (Fig. 3b) after annealing at 350°C showed that all observed reflections were from zinc oxide. The 0001 peak was several times as strong as the 1000 and 1010 peaks. The relative intensities differ from the calculated intensities (1000, 57%; 0001, 44%; 1010, 100%), indicating a *c*-axis texture.

### *Seeded Growth*

Guo et al. [18] reported the deposition of ZnO nanoparticles from a colloidal solution. Such particles, however, readily aggregate and loosely adhere to the substrate surface. Their surface is covered with significant amounts of adsorbed reactants, which have an adverse effect on the luminescent properties of the particles.

The acetate route used in this study to produce zinc oxide nanoparticles enables the growth of a thin seed layer textured along the rapid growth axis of zinc oxide. Nucleation occurs directly on the substrate surface, ensuring adequate surface adhesion. This method enables one to improve nanorod alignment and reduce the effect of the seed layer on the luminescent and transport properties of ZnO nanorods.

Using chemical precipitation from solution, and seeds produced on substrates by the acetate route, we grew a nanorod array. Since the seeds were *c*-axis textured, the samples had no polycrystalline, imperfect layer, as evidenced by SEM results (Fig. 3c). An imperfect layer is a layer formed by nanorods growing from orientation-disordered nanoseeds. Such nanorods begin to grow in various directions. Their growth is suppressed by intersections of the nanorods in the initial stage of disordered growth. As a result, growth proceeds in only one direction, vertical, but it yields a

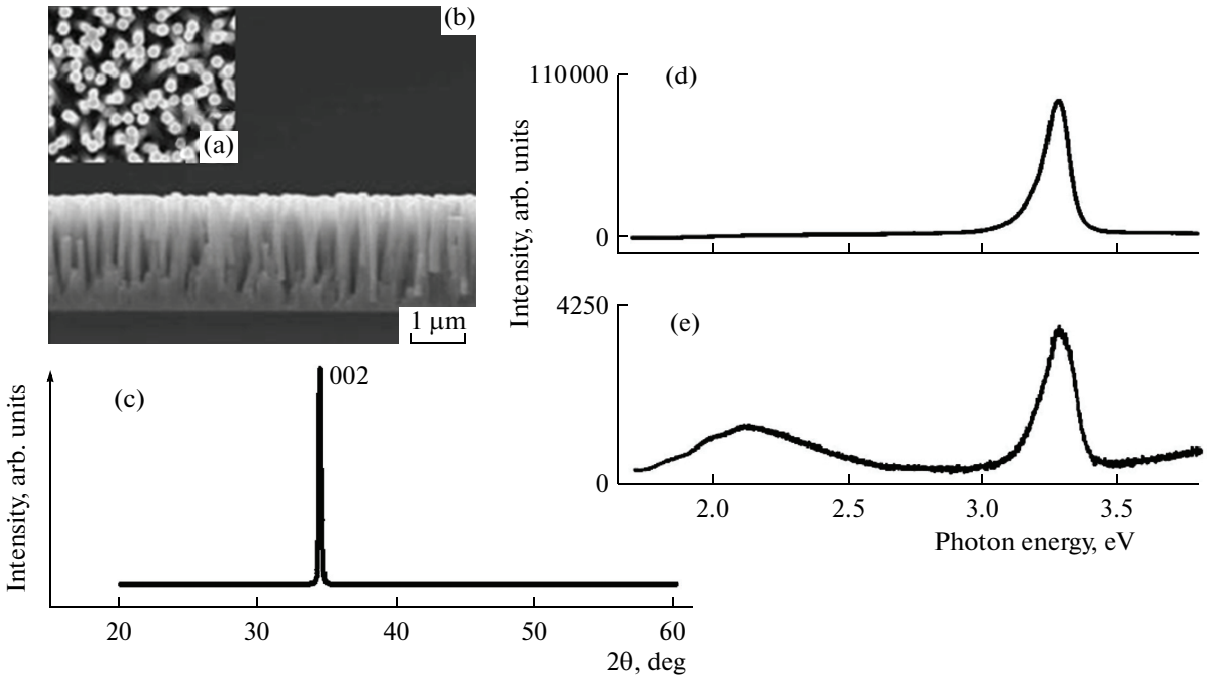


**Fig. 4.** SEM micrographs of a sample grown on a substrate with a seed layer: (a) top view, (b) side view; (c) XRD pattern of nanorods produced by seeded vapor growth; (d, e) photoluminescence spectra of ZnO nanorods produced by seeded and unseeded growth, respectively.

polycrystalline layer which may reach several hundred nanometers in thickness.

Figure 4b shows SEM micrographs of nanorods produced by chemical vapor deposition on a substrate with a seed layer. The substrate was placed in position 2 in the growth zone (Fig. 1a). According to the SEM results, the nanorods are 2 μm in height and 180 nm in average diameter. Because the seeds are oriented in the [0001] direction, the sample has no polycrystalline layer. The XRD pattern of the sample grown on textured seeds (Fig. 4c) shows only one reflection, 002. This lends support to the conclusion drawn from SEM data that zinc oxide seeds increase the degree of alignment of nanorods.

To find out how seeds influence the optical properties of the samples, we measured their photoluminescence spectra. The spectra are shown in Figs. 4d and 4e. The spectrum of the sample produced by unseeded growth shows a strong green luminescence band centered at ≃2.13 eV and UV luminescence peaking at ~3.28 eV, corresponding to free exciton recombination. The green emission band is commonly attributed to high concentrations of oxygen vacancies and other defects [18]. The peak intensities of the UV and yellow bands are in the ratio ≃2.5 : 1. The spectrum of the sample grown on a seed layer shows only the UV band, centered at ≃3.28 eV, with no defect-related emission band. The UV luminescence intensity is considerably higher in the latter sample compared to the former. These data lead us to conclude that the samples produced by seeded growth contain much less defects because they have no polycrystalline layer.

### *Oriented Nanorod Growth*

To grow nanorods on seeds applied locally to a surface, it is necessary to establish synthesis parameters that would allow secondary nucleation to be suppressed. Nanorods will then grow only on seeds.

Crystal growth from solution requires supersaturation. Strong supersaturation leads to a higher probability of homogeneous nucleation because, with increasing supersaturation, both the work of formation of a nucleus and the critical nucleus size, $r_c \sim 1/\Delta\mu$, decrease [19]. Only those nuclei will be able to stably grow which are more than $r_c$ in size. Zinc oxide growth from solution at elevated temperatures is due to the thermolysis of a zinc ethylenediamine complex and the incorporation of the released zinc cations into the growing crystal:

$$[Zn(en)_x(OH)_y]^{2-y} \rightarrow Zn^{2+} + x\,en + y\,OH^-, \quad (4)$$

$$Zn^{2+} + 2OH^- \rightarrow ZnO + H_2O. \quad (5)$$

Clearly, in the system under investigation the key factor determining the supersaturation is temperature. To suppress secondary nucleation, the temperature should ensure a sufficiently low decomposition rate of the zinc ethylenediamine complex $[Zn(en)_x(OH)_y]^{2-y}$. The $Zn^{2+}$ concentration in the system will then be constant, the supersaturation will be low, the work of

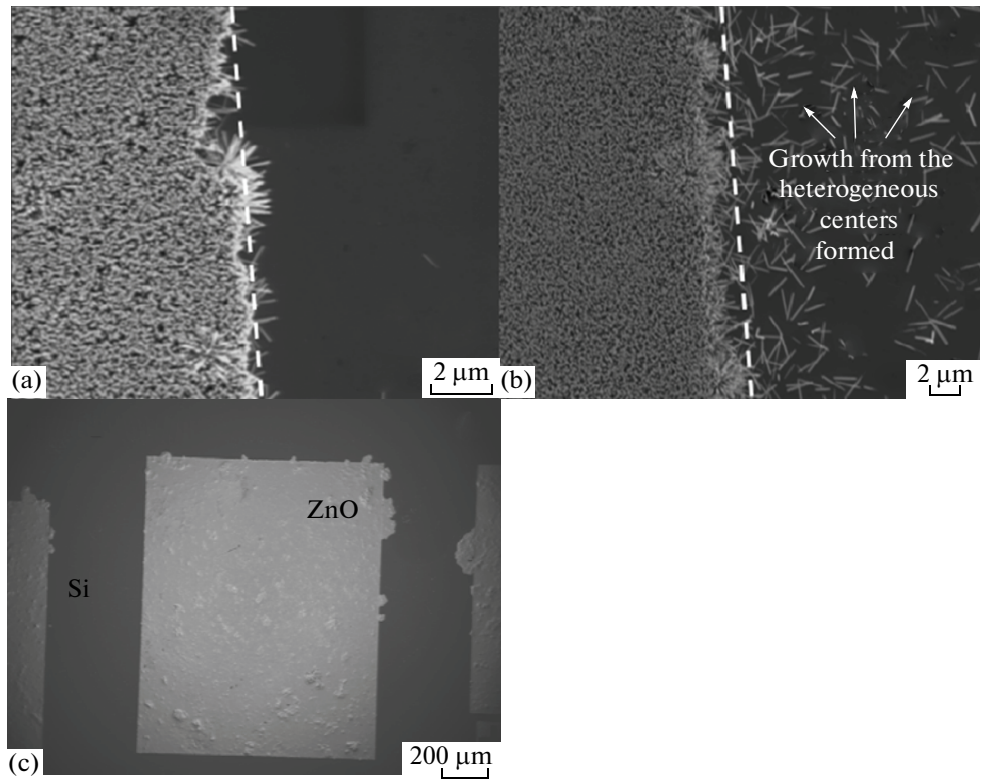


**Fig. 5.** ZnO nanorods on substrates with a photoresist mask: growth temperature of (a) 80 and (b) 110°C; (c) nanorod arrays 1 × 1 mm in dimensions.

nucleation will increase, and growth on seeds will be more energetically favorable. Varied experimentation has shown that this condition is met in the temperature range 80–110°C.

**Growth on substrates with photoresist.** WE developed a procedure for applying ZnO seeds to a substrate in the form of squares 1 × 1 mm in dimensions (Fig. 5c), which corresponds to a photoresist mask pattern.

Figures 5a and 5b are SEM micrographs of ZnO nanorods grown on seeds through chemical precipitation from solution at 80 and 110°C. The dashed lines represent the initial boundary of the photoresist mask. On both samples, we observe oriented nanorod growth on seeds, but the sample synthesized at the higher temperature contains a significant concentration of heterogeneous growth centers formed during synthesis. These results lend support to the above hypothesis that the temperature influences the growth directionality: low supersaturations in the system can be reached at lower temperatures. Thus, the optimal temperature for local growth of nanorod arrays is 80°C (crystals grown at lower temperatures had markedly poorer optical and transport properties, so we did not examined temperatures below 80°C). Owing to the acetate route used to prepare seeds, the arrays have a high degree of alignment perpendicular to the substrate.

The key parameters influencing the supersaturation during vapor growth of nanocrystals are the gas (argon and oxygen) flow rate, the temperature gradient in the reactor, and the zinc source temperature. Theoretically, an optimal combination of these parameters can be found in order to inhibit the formation of heterogeneous growth centers. However, the mass transport in the system under consideration occurs under complex gas-dynamic conditions, and the properties of nanorods may vary significantly even within one substrate. Optimal conditions for oriented growth may vary from region to region. In connection with this, we have shown that oriented nanorod growth from solution has important advantages.

## CONCLUSIONS

A layer of *c*-axis-oriented seed nanocrystals produced on a substrate considerably improves the alignment of both solution- and vapor-grown nanorod arrays. The use of such seeds markedly increases the UV luminescence intensity and reduces the defect-related luminescence intensity.

The proposed novel technique for photoresist removal after producing a zinc acetate film allows one to apply the process for the preparation of textured seeds to patterned substrates and to produce highly aligned arrays in local surface areas.

## REFERENCES


1. Heo, Y.W., Norton, D.P., Tien, L.C., et al., ZnO Nanowire Growth and Devices, *Mater. Sci. Eng., R,* 2004, vol. 47, pp. 1–47.
2. Law, M., Greene, L., Johnson, J., et al., Nanowire Dye-Sensitized Solar Cells, *Nat. Mater.,* 2005, vol. 4, pp. 455–459.
3. Wang, Z.-L., Piezoelectric Nanogenerators Based on Zinc Oxide Nanowire Arrays, *Science,* 2006, vol. 312, pp. 242–246.
4. Kim, H.S., Lugo, F., Pearton, S.J., and Norton, D.P., Phosphorus Doped ZnO Light Emitting Diodes Fabricated via Pulsed Laser Deposition, *Appl. Phys. Lett.,* 2008, vol. 92, pp. 108–112.
5. Martinson, A.B.F. et al., ZnO Nanotube Based Dye-Sensitized Solar Cells, *Phys. Chem. Chem. Phys.,* 2006, vol. 8, pp. 4655–4659.
6. Baranov, A.N. et al., Growth of ZnO Nanorods From a Salt Mixture, *Nanotechnology,* 2005, vol. 16, p. 1918.
7. Znaidia, L., Soler Illia, G.J.A.A., Benyahia, S., et al., Oriented ZnO Thin Films Synthesis by Sol–Gel Process for Laser Application, *Thin Solid Films,* 2003, vol. 428, pp. 257–262.
8. Shan, F.K. and Yu, Y.S., Substrate Effects of ZnO Thin Films Prepared by PLD Technique, *J. Eur. Ceram. Soc.,* 2004, vol. 24, pp. 1869–1872.
9. Chang, P.C. et al., ZnO Nanowires Synthesized by Vapor Trapping CVD Method, *Chem. Mater.,* 2004, vol. 16, p. 5133.
10. Liu, Z. et al., Growth of ZnO Nanorods by Aqueous Solution Method with Electrodeposited ZnO Seed Layers, *Appl. Surf. Sci.,* 2009, vol. 255, p. 6415.
11. Greene, L.E. et al., General Route to Vertical ZnO Nanowire A*rrays Using Textured ZnO Seeds, Nano Lett,* 2005, vol. 5, pp. 1231–1236.
12. *Spravochnik khimika* (Chemist's Handbook), Nikol'skii, B.P., Ed., Moscow: Khimizdat, 1952, vol. 2, pp. 254–255.
13. Red'kin, A.N., et al., Elemental Vapor-Phase Synthesis of Nanostructured Zinc Oxide, *Inorg. Mater.,* 2009, vol. 45, no. 11, pp. 1246–1251.
14. Kotova, O., et al., Gas-Phase Synthesis of Lanthanide(III) Benzoates $Ln(Bz)_3$ (Ln = La, Tb, Lu), *Russ. J. Coord. Chem.,* 2007, vol. 33, no. 6, pp. 454–457.
15. Wei, M., Zhi, D., and MacManus-Driscoll, J.L., Self-Catalysed Growth of Zinc Oxide Nanowires, *Nanotechnology,* 2005, vol. 16, pp. 1364–1368.
16. Greenwood, N.N. and Earnshaw, A., *Chemistry of the Elements,* Oxford: Butterworth,, 1997. Translated under the title *Khimiya elementov,* Moscow: BINOM, Laboratoriya Znanii, 2008, vol. 2, p. 536.
17. Baruah, S. and Dutta, J., Hydrothermal Growth of ZnO Nanostructures, *Sci. Technol. Adv. Mater.,* 2009, vol. 10, pp. 1–13.
18. Guo, M., Diao, P., and Cai, S., Hydrothermal Growth of Perpendicularly Oriented ZnO Nanorod Array Film and Its Photoelectrochemical Properties, *Appl. Surf. Sci.,* 2005, vol. 249, pp. 71–75.
19. Petrov, T.G., Treivus, E.B., Punin, Yu.O., and Kasatkin, A.P., *Vyrashchivanie kristallov iz rastvorov* (Crystal 1 Growth from Solutions), Leningrad: Nedra, 1983, 2nd ed., p. 200.
20. Govender, K., Boyle, D.S., Kenway, P.B., and O'Brien, P., Understanding the Factors That Govern the Deposition and Morphology of Thin Films of ZnO from Aqueous Solution, *J. Mater. Chem.,* 2004, vol. 14, pp. 25–75.


SPELL: OK